

Study of the Toxicity and Cell Viability of Zirconium Oxide Nanoparticles Prepared from an Extract of the Vitex Agnus Castus plant

Saba H. Mahdi ¹, Lekaa K. Abdul karem ^{*2}

¹ Ministry of Education, Directorate of Education Rusafa First, Iraq.

² Departments of Chemistry, College of Education for Pure Sciences Ibn Al-Haitham, University of Baghdad, Iraq.

*Corresponding Author.

Received 07/10/2023, Revised 12/01/2024, Accepted 14/01/2024, Published Online First 20/09/2024



© 2022 The Author(s). Published by College of Science for Women, University of Baghdad.

This is an open access article distributed under the terms of the [Creative Commons Attribution 4.0 International License](https://creativecommons.org/licenses/by/4.0/), which permits unrestricted use, distribution, and reproduction in any medium, provided the original work is properly cited.

Abstract

In the current study, ZrO₂ nanoparticles were synthesized using a plant extract derived from Vitex agnus castus, and an alkaline medium such as sodium hydroxide. A biosynthetic approach was utilized to prepare zirconium oxide nanoparticles for this research project. This method stands out from others due to its cost-effectiveness, simplicity, and lack of potential risks. The prepared samples were characterized using transmission electron microscopy TEM, scanning electron microscopy SEM, Fourier transform infrared spectroscopy FT-IR, ultraviolet-visible spectroscopy UV-VIS, X-ray diffraction, and energy-dispersive X-ray spectroscopy EDX. The size of the crystal was determined using X-ray diffraction in conjunction with the Debye-Scherrer equation, resulting in a value of 26.37 nm. Scanning electron microscopy and transmission electron microscopy were employed to ascertain the particle size of ZrO₂ nanoparticles. In this study, these nanoparticles exhibited varying levels of activity against two types of gram-positive bacteria (*Staphylococcus aureus* and *Streptococcus pneumonia*), two types of gram-negative bacteria (*Proteus mirabilis* and *Escherichia coli*), and one type of fungus, *Candida*. Interestingly, synthesized zirconium oxide nanoparticles' anticancer potential has been uncovered with MTT assays at varied concentrations for cell line A549 lung cancer. The percentage of inhibition revealed an increase with increasing concentration. Calculating the inhibition of half of the cells IC₅₀, which was equal to (58.4 mg/ml), suggests that zirconium oxide nanoparticles have the potential for utilization in cancer treatment.

Keywords: Antibacterial, Biosynthesis approach, Cell line A549, Nanoparticles, Zirconium oxide.

Introduction

Manipulating the size and shape of structures, electronics, and other systems within the nanoscale, ranging from 1 nanometer to 100 nanometers, is referred to as nanotechnology^{1,2}. Because of their small size, nanostructures exhibit significantly larger surface areas compared to their bulk counterparts. This increased surface area enhances their reactivity and allows for greater control over numerous features³⁻⁵.

Due to their unique characteristics, nanoparticles (NPs) are increasingly used in various industries, such as biomedicine, cosmetics, electronics, food

analysis, environmental and remediation, and paints⁶⁻⁸. The field of nano-scale science and engineering facilitates an enhanced understanding and manipulation of materials at the atomic and molecular scales⁹. The remarkable electrical, optical, and magnetic properties of nano-size particles have garnered significant attention in academic discourse¹⁰.

These nanoparticles exhibit dimensions that make them suitable candidates for nanotechnology^{11,12}. Nevertheless, it is crucial to acknowledge that these nanoparticles' dimensions may negatively

affect human health and the environment. While the physical synthesis approach incurs high costs, the chemical synthesis method involves the use of hazardous substances¹³.

To address environmental concerns, scientists have developed an environmentally sustainable and ecologically sound approach to synthesizing nanoparticles, harnessing the potential of microbes and plants. Various plant components, including leaves, stems, roots, shoots, flowers, barks, seeds, and their metabolites, have proven effective in nanoparticle synthesis¹⁴⁻¹⁷. Plants known for their cost-effectiveness and eco-friendliness, offer sophisticated solutions beneficial for human utilization.¹⁸

Vitex agnus-castus, commonly known as vitex, chaste tree, Abraham's balm, or monk's pepper, originates from the Mediterranean region. Although the *Vitex* genus primarily includes tropical and subtropical flowering plants, only a limited number

Materials and Methods

The process of collecting specimens or samples for scientific analysis involved using zirconium sulphate in conjunction with *Vitex agnus-castus* sourced from a nearby location. NaOH was acquired from the Indian company, Alpha Chemica, and ZrSO₄ was utilized. The experimental setup included a magnetic stirrer and a sensitive electronic balance model, specifically 220C1.

The chemicals underwent creation and identification through various spectroscopic and microscopic techniques, such as the PLC centrifuge, the electric oven model (FAITHFUL) - WHL 25 AB, and the FT-IR (8500S) spectroscopic technique covering the wave number range of 400-4000 cm⁻¹. X-ray diffraction analysis was conducted using a PW1730 instrument manufactured by Phillips/Holland. The pH of the samples was measured using a UV-visible tape measure of the PH-type (160/UV) from Shimadzu, all of which were located at the center of examinations.

For energy-dispersive X-ray spectroscopy (EDX) purposes, an X-ray energy dispersion device, specifically the scanning electron microscope (SEM) FESEM-EDS Model MIRAI manufactured by TESCAN in the Czech Republic, was employed. The observation of the utilization of Transmission Electron Microscopes (TEM) equipped with the model designation EM10C-100Kv was noted.

Preparation of plant extract

of species inhabit temperate zones¹⁹. Previous studies have indicated that the antibacterial efficacy of several extracts from various parts of the pomegranate plant against human infections is moderate²⁰. Extensive research has documented the versatile applications of zirconium oxide (ZrO₂) spanning adsorption, photo-degradation, antibacterial properties, and structural reinforcement. Zirconium, a transition metal, exhibits improved mechanical, thermal, catalytic, and corrosion-resistant properties²¹. Various methodologies were employed to assess the antioxidant capacity of the acquired Zr-NPs²². The primary objective of this work is to prepare zirconium oxide nanoparticles through green synthesis, utilizing a plant extract derived from *Vitex agnus castus*. Furthermore, the study aims to evaluate the antimicrobial activity and toxicity of the synthesized nanoparticles.

After thorough rinsing with tap water to eliminate any residual impurities, the fresh herbs were dried sufficiently, first by removing excess water and then by being left to air dry overnight. Following this, the material was pulverized to facilitate the subsequent extraction procedure.

To initiate the extraction, 20 g of the herbs were added to 200 milliliters of deionized water. The resulting mixture underwent continuous stirring with a magnetic stirrer for thirty minutes while maintaining a temperature range of sixty to seventy degrees Celsius as shown in Fig. 1. Subsequently, the mixture was allowed to cool naturally to room temperature before being discarded. The filtration process was carried out using a centrifuge apparatus. The plant extract was placed in test tubes and centrifuged at 4000 revolutions per minute. This centrifugation step was crucial to eliminate any residual debris and fibers while preserving the filter's integrity²³.

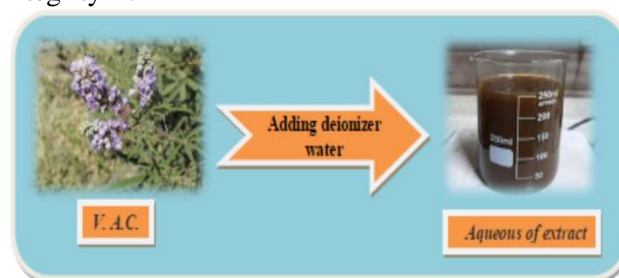


Figure 1. Preparation of plant extracted solution

Preparation of ZrO₂ NPs

The manufacture of zirconium oxide (ZrO₂) nanoparticles was conducted using an environmentally sustainable method. After stirring for 30 minutes, 100 milliliters of filtered plant extract solution were combined with an equal volume of aqueous vanadium sulphate solution, with a concentration of 1.63g per 100 milliliters. Subsequently, 50 milliliters of sodium hydroxide solution containing 2 g, were gradually added to the system until the pH level reached 12. After sixty minutes at a temperature of seventy degrees Celsius, a noticeable change in colour was observed, indicating the formation of a precipitate. Following an undisturbed overnight period, the substance underwent separation through a centrifuge. The specimens were then subjected to repeat rinsing with deionised water as shown in Fig. 2 and dried in an electric oven at a temperature of 300 degrees Celsius for three hours.

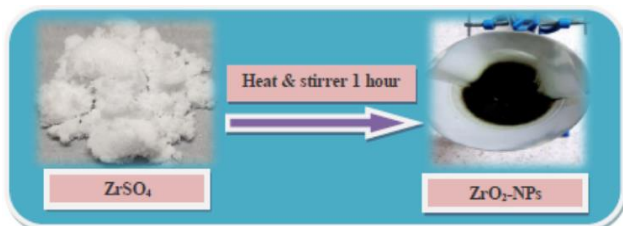


Figure 2. Preparation of ZrO₂ NPs

Results and Discussion

FTIR Spectrum analysis

The presence of the Zr-O bond is evident within the ZrO₂ structure, as indicated by the bands in the wave number range of 425-640.37 cm⁻¹ in the Fourier Transform Infrared (FTIR) spectra of ZrO₂, illustrated in Fig.3. Specifically, the absorption bands at 2032.37 cm⁻¹ due to aliphatic bond of C=C

Characterization

Antimicrobial Activity

The synthesized ZrO₂ nanoparticles were assessed for their antibacterial activity against two reference bacterial strains, namely *Staphylococcus aureus*, *Streptococcus pneumonia* (Gram-positive), and *Escherichia coli*, *Proteus mirabilis* (Gram-negative), as well as the fungal strain *Candida albicans*. This assessment was conducted using the disc diffusion method on Muller Hinton agar nutritional medium. An identical procedure was implemented to evaluate the antifungal efficacy, utilizing a nutrient medium (agar).

Cytotoxic Assays

The effectiveness of nanoparticles against colon cancer cells and their impact on the cellular activity were assessed using the MTT assay. The calorimetric technique was used to analyze the metabolic activity of the cells, and the results from this test were employed to determine the efficacy of the nanoparticles.

bending vibration, while the bands at 1625.69 and 1552.16 cm⁻¹ correspond to the C=O and C=C bending vibrations respectively, these peaks may be evidence for organic impurities. The peak at 1242 cm⁻¹ is assigned to C-O bending vibration within the ZrO₂ structure^{24, 25}.

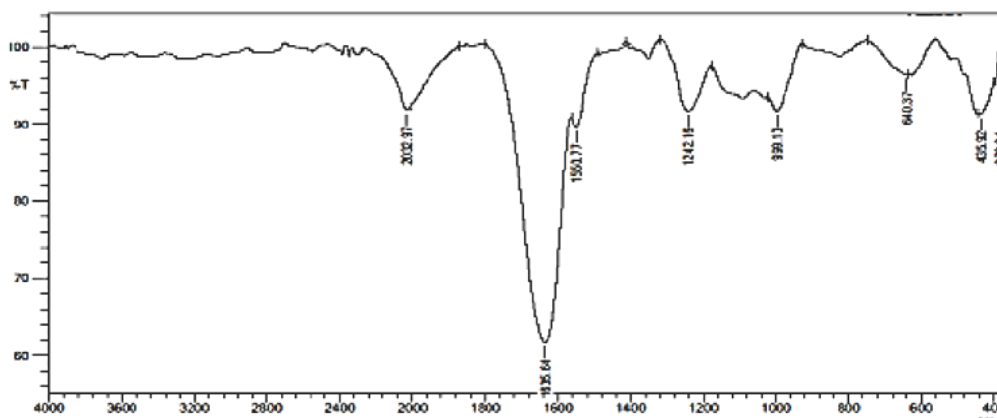


Figure 3. The FTIR of ZrO₂ NPs

The UV-Visible spectrum

The optical properties of the nanoparticles synthesized through the utilization of plant extract and vanadium sulphate were analyzed using the ultraviolet-visible spectroscopy technique, as illustrated in the accompanying images. Ultraviolet-visible (UV-vis) radiation represents a specific range within the electromagnetic spectrum, characterized

by wavelengths shorter than visible light. Ultraviolet (UV) rays encompass a broader spatial range than X-rays. Fig. 4 depicts the UV-Vis absorption spectrum of ZrO₂ NPs biosynthesized. The appearance of the absorption peak at 356.0 nm in this spectrum is attributed to the transition of holes between Zr and O, indicating a distinctive feature of the biosynthesis process.

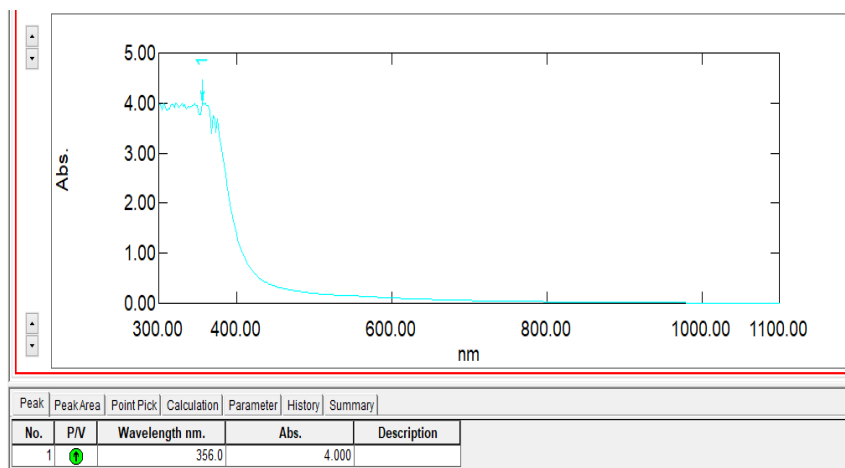


Figure 4. UV-Vis spectrum of ZrO₂ NPs

X-ray diffraction (XRD) analysis

The X-ray diffraction (XRD) analysis reveals that the orthorhombic ZrO₂ crystal structure exhibits diffraction peaks corresponding to various crystal planes, including (111), (002), (022), (100), (120), (111), (200) and (211). These peaks are observed at 2θ angles of 16.3751°, 18.8804°, 23.5438°, 26.2517°, 34.2207°, 38.1606, 49.0097°, and 59.0104°, respectively. Identification of these crystal planes is based on the JCPDS card (no. 44-0141)²⁶. Notably, the X-ray diffraction (XRD) examinations conducted on the ZrO₂ (NPs) sample revealed the absence of impurity peaks, indicative of a high degree of crystalline.

The Debye-Scherrer's equation ($D = 0.9 \lambda / \beta \cos \theta$) was employed to determine the average size of the crystals. In this equation, D represents the average crystalline size, λ denotes the wavelength of Cu K X-ray radiation ($\lambda = 1.5418 \text{ \AA}$). The obtained value was determined to be 26.37 nm, as depicted in Fig. 5 and outlined in Table 1.

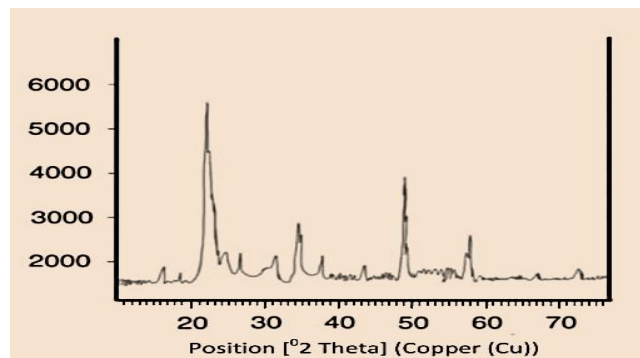


Figure 5. XRD of ZrO₂ NPs

Table 1. The data of XRD for ZrO₂ NPs.

Pos. [°2Th.]	Height [cts]	FWHM [°2Th.]	Particle size (nm)	Average crystal size (nm)
16.3751	188.47	0.2432	34.50	26.37
18.8804	614.50	0.258	32.63	
23.5438	3039.56	0.258	32.88	
26.2517	5963.14	0.2943	28.97	
34.2207	1061.55	0.3442	25.24	
38.1606	2155.46	0.579	15.18	
49.0097	825.46	0.3966	27.79	
58.0104	512.50	0.4521	13.79	

EDX analysis

In the energy-dispersive X-ray (EDX) spectra of ZrO_2 nanoparticles, zirconium and oxygen exhibit the anticipated peaks, as illustrated in Fig. 6 while maintaining a one-to-one ratio between them. The results demonstrate the high purity level evident in the synthesized nanoparticles. The results obtained from the EDX experiment align closely with basic theoretical calculations, providing robust and consistent estimates²⁷.

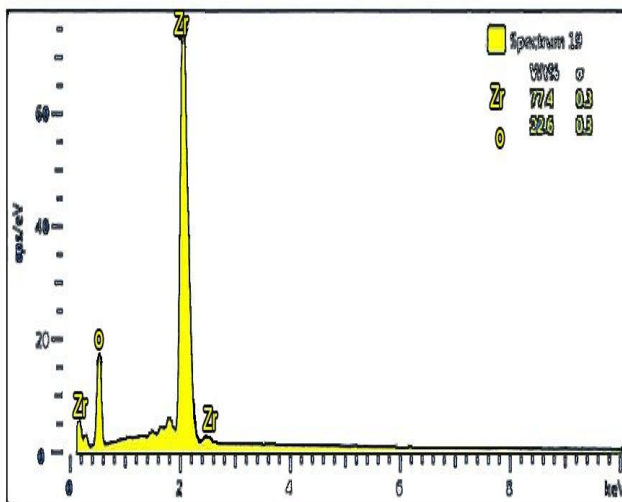


Figure 6. EDX of ZrO_2 NPs.

SEM and TEM analysis

The morphology and structure of the nanomaterial were determined through scanning electron microscopy (SEM) and transmission electron microscopy (TEM). The analyses conducted in Figs. 7,8 using SEM and TEM indicate the presence of a limited quantity of spherical-shaped ZrO_2 nanoparticles (NPs) with a nano structured, unconsolidated morphology.

The TEM image analysis further reveals that the ZrO_2 nanoparticles exhibit a nano-scale structure that lacked consolidation. It is essential to acknowledge that the samples contain significant pore content, making them well suited for adsorption applications²⁸. The TEM image also demonstrates a high packing density of ZrO_2 nanoparticles in the sample. The sample exhibits zero-dimensional spherical structural properties, with all dimensions at the nano-scale. This characteristic is highly desirable in the chemical nature of nanomaterials. However, due to limitations in measurement accuracy, the exact shape of the sample cannot be definitively determined²⁹.

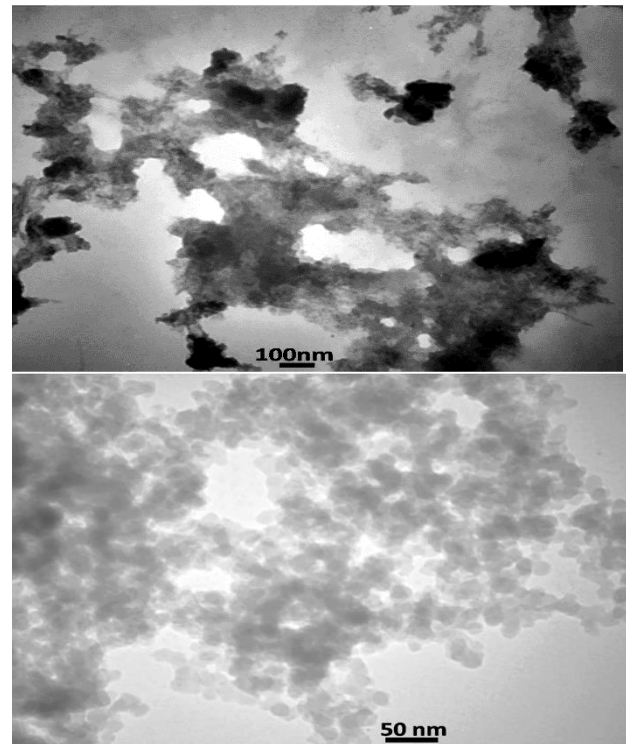


Figure 7. TEM of ZrO_2 NPs

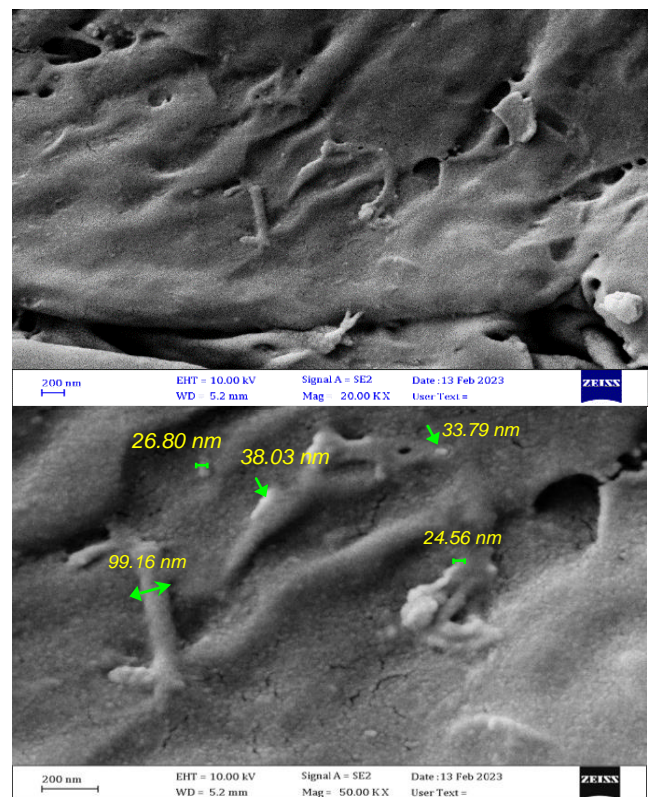


Figure 8. SEM of ZrO_2 NPs

Antimicrobial Studies

In this study, the synthesized ZrO_2 was evaluated against a total of four bacterial strains, including

(*Staphylococcus aureus* and *Streptococcus pneumoniae* (both Gram-positive), as well as *Proteus mirabilis* and *Escherichia coli* (both Gram-negative). Additionally, one fungal strain (*Candida*) was included in the assessment. The well plate method on nutritional agar was employed to study the effect of zirconium oxide nanoparticles on organism pouring (20-25ml) in Nutrient Agar Medium for each Petri dish^{30, 31}. A Nutrient Agar was prepared in a Mast by dissolving (37.5 gm) of the powder in a Liter of distilled water, and with a pH (7.3), then, it was sterilized by using Auto Cleave. This medium is used to grow organism, maintaining strains, and studying the antagonistic activity of ZrO_2 towards the isolates used in the study.

The biological activity of the Nano oxide was measured in millimeters (mm) by assessing the diameter of the inhibition zone (ZI) surrounding each aperture, with dimethyl sulfoxide (DMSO) employed as the solvent³²⁻³⁴. After becoming cold, the Petri dish was kept in an incubator for 24 hours

and in a temperature 37 °C to prevent these Petri dishes from being polluted. Then, the Petri dish was soaked in 10 ml of the prepared organism as it had been mentioned in the previous paragraph and which contained (1.5 x 810 cell/ml), then, they were diffused equally on the surface of the Nutrient Agar Medium by using glass spreader^{35,36}. A hole was made on the surface of the cultured medium by using cork borer. Then, nanoparticles of 100 micro ml were put in each hole leaving one of these holes to be the control hole, which only contained the used solvent (DMSO). The Petri dish was kept in the refrigerator for half an hour at a temperature 4 °C; then, the Petri dish was incubated in a temperature 37 °C for 24 hours. The experimental results demonstrated differences in the antimicrobial effectiveness of the Nano oxide against four distinct types of bacteria and fungus. The high activity of ZrO_2 is shown against the fungal *Candida*. These findings are presented in Table 2, chart 1.

Table 2. The Zone Inhibition in (mm) of ZrO_2 NPs against Different Microbial

Compound	<i>Staphylococcus aureus</i>	<i>Streptococcus pneumoniae</i>	<i>Escharia coli</i>	<i>Proteus mirabilis</i>	<i>Candida albicans</i>
DMSO	----	----	----	----	----
ZrO_2 NPs	22	25	17	23	29

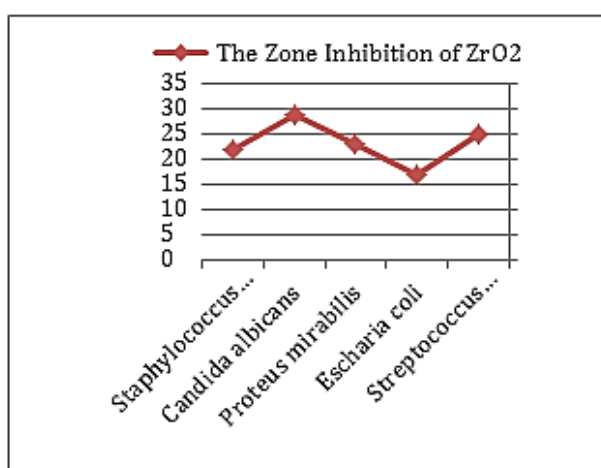


Chart 1. The Antibacterial activity of ZrO_2 NPs

Viability and Cytotoxicity of Cells Utilizing Assays (MTT)

The experimental approach in this study involved utilizing the A549 lung cancer cell line. The dye known as 3-(4, 5-dimethylthiazol-2-yl)-2,5-diphenyl tetrazolium bromide (MTT), commonly used in cell

viability assays for its characteristic hue, was employed to assess cell vitality^{37,38}.

The findings of this study indicate a notable cytotoxic impact of the zirconium oxide on cancer cells. The subsequent section will provide a comprehensive explanation of the aforementioned topic. The present study aimed to assess the extent of the harmful impact by determining the percentage of growth inhibition rate (referred to as the Inhibition Rate) over 24 hours at a temperature of 37°C.

The data presented in Table 3 reveals that the A549 lung cancer cell line exhibited the highest inhibition percentage (17.43%) when treated with the synthesized nanoparticles at a dose of 500 µg/ mL. The findings suggest that the concentration of the substance used plays a crucial role in determining the extent of cell inhibition. The study further disclosed that an elevated concentration levels result in a decrease in viability percentage, subsequently increasing the inhibition percentage of cell growth in the malignant cell line. This relationship is demonstrated in both Table. 3 and Chart 2^{37, 38}.

Table 3. Statistical values of A549 lung cancer cell line of ZrO₂NPs

Concentration mg/ml	Relative Cell Viability %	Number of Values	Standard deviation
Control	100	8	0.027
7.81	94.50	8	0.024
15.625	87.31	8	0.027
31.25	65.01	8	0.025
62.5	42.65	8	0.023
125	33.20	8	0.028
250	28.65	8	0.025
500	17.34	8	0.022

the A549 cancer cell line is the determination of the half-inhibition concentration (*IC*₅₀). This concentration, represented by *IC*₅₀³⁹⁻⁴², has the capability of causing the death of approximately 50% of the cells. The investigation into the interaction between nanoparticles and a lung cancer cell line revealed a notable outcome. Specifically, the half inhibitory concentration was established at 58.4 µg/mL, indicating a highly favourable result. This suggests that zirconium nanoparticles derived from the *Vitex agnus castus* extract can effectively eliminate lung cancer cells⁴³. The findings of this study bear substantial importance for the potential application of selective treatment for colon cancer, as illustrated in Table 3 and Fig. 9.

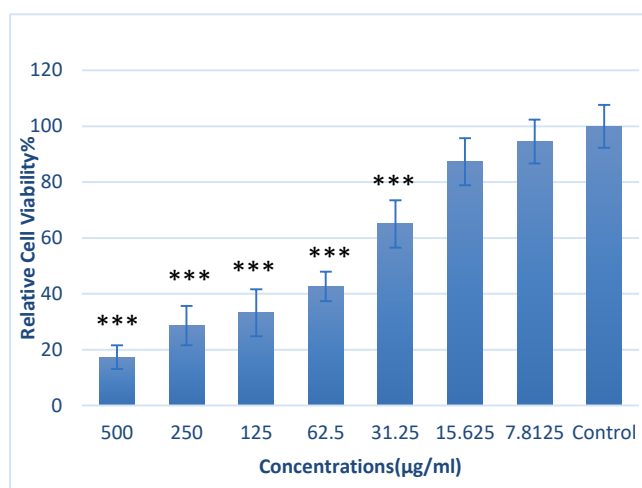


Chart 2. The percentage of viability in the cells of the cancer cell line A549 of ZrO₂ NPs

Fifty percent inhibition of ZrO₂-NPs

One of the significant findings arising from the conducted tests on zirconium oxide nanoparticles on

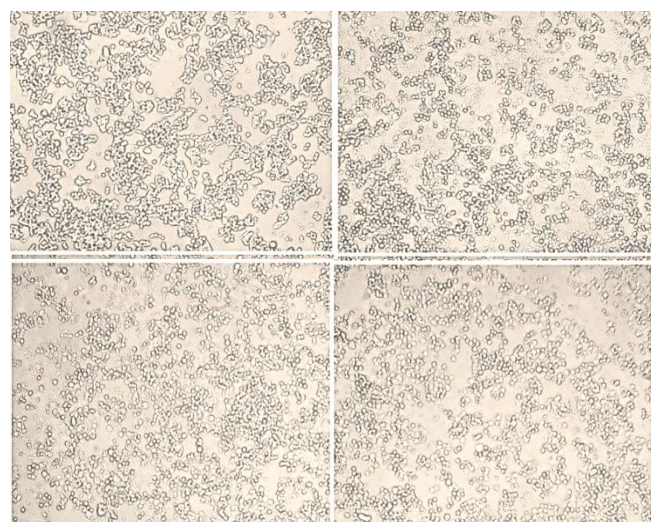


Figure 9. Cancer cells treated with ZrO₂NPs at different concentrations after addition

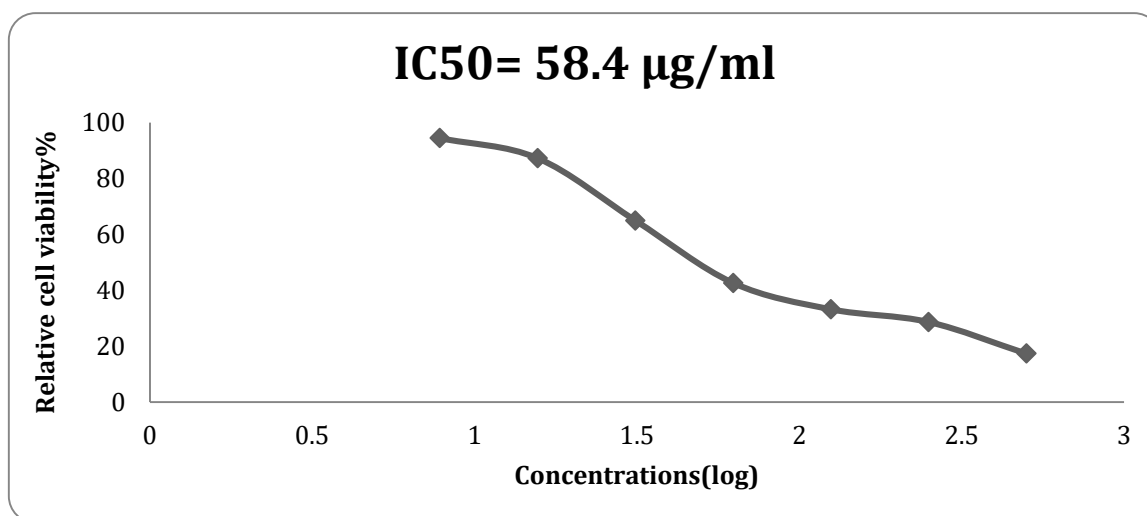


Figure 10. Determining the half-inhibition concentration (*IC*₅₀)

Conclusion

The synthesis of zirconium oxide nanoparticles was achieved through a sustainable method, involving the use of *Vitex agnus castus* extract and $ZrSO_4$. The resulting crystals exhibited a mono crystalline structure with a diameter of 26.37 units. These particles demonstrated varying levels of activity against four distinct bacterial strains, comprising two gram-positive strains (*Staphylococcus aureus*, *Streptococcus pneumoniae*) and two gram-negative

strains (*Proteus mirabilis*, *Escherichia coli*). Additionally, the particles exhibited significant efficacy against *Candida*, a type of fungus, showing the highest level of activity. On the other hand, the toxicity of the nano-oxide was evaluated on the A549 lung cancer cell line, revealing an average inhibition of *IC50* cells at a concentration of 58.4 mg/ml. The outcomes of this study hold significant importance for the potential application of targeted therapy for lung cancer.

Acknowledgment

Sincere thanks are extended by the author to the Chemistry Department and College of Education for Pure Sciences at Ibn-Al Haitham University in

Baghdad, Iraq, for providing the resources necessary for the completion of this research project.

Authors' Declaration

- Conflicts of Interest: None.
- We hereby confirm that all the Figures and Tables in the manuscript are ours. Furthermore, any Figures and images, that are not ours, have been included with the necessary permission for re-publication, which is attached to the manuscript.
- Authors sign on ethical consideration's approval.

- No animal studies are present in the manuscript.
- No potentially identified images or data are present in the manuscript.
- Ethical Clearance: The project was approved by the local ethical committee at University of Baghdad.

Authors' Contribution Statement

Our participation in the research project named "Study of the Toxicity and Cell Viability of Zirconium Oxide Nanoparticles Prepared from an Extract of the Vitex Agnus Castus plant" has been confirmed by S.H. M. and L. K. A. Our contributions

covered a wide range of areas, such as the conception and design of the study, the collection of data, the analysis and interpretation of that data, and the preparation of the paper, as well as its following revisions and edits

References

1. Farooqi ZUR, kQadeer A, Hussain MM, Zeeshan N, Ilic P. Characterization and physicochemical properties of nanomaterials. In *Nanomaterials: Synthesis, Characterization, Hazards and Safety*; A volume in Micro and Nano Technologies, Elsevier. 2021; 97-121. <https://doi.org/10.1016/C2020-0-00287-2>.
2. Varghese RJ, Parani S, Thomas S, Oluwafemi OS, Wu J. Introduction to nanomaterials: synthesis and applications. In *Nanomaterials for Solar Cell Applications*; Elsevier. 2019; 75-95. <https://doi.org/10.1016/C2016-0-03432-0>
3. Barik TK, Maity GC, Gupta P, Mohan L, Santra TS. *Nanomaterials: An Introduction. Nanomaterials and Their Biomedical Applications*. 2021; 1-27. https://doi.org/10.1007/978-981-33-6252-9_1
4. Singh B K, Lee S, Na K. An overview on metal-related catalysts: metal oxides, nanoporous metals and supported metal nanoparticles on metal organic frameworks and zeolites. *Rare Metals*. 2020; 39: 751-766. <https://doi.org/10.1007/s12598-019-01205-6>.
5. Salem SS, Fouda MMG, Fouda A, Awad MA, Al-Olayan EM, Allam AA, et al. Antibacterial, Cytotoxicity and Larvicidal Activity of Green Synthesized Selenium Nanoparticles Using *Penicillium corylophilum*. *J Clust Sci*. 2021; 32: 351-361. <https://doi.org/10.1007/s10876-020-01794-8>
6. Khan S, Mansoor S, Rafi Z, Kumari B, Shoaib A, Saeed M, et al. A review on nanotechnology: Properties, applications, and mechanistic insights of cellular uptake mechanisms. *J Mol Liq*. 2021; 118008. <https://doi.org/10.1016/j.molliq.2021.118008>

7. Al-Bahadili Z R, AL-Hamdani AAS, Rashid FA, Al-Zubaidi LA, Ibrahim SM. An Evaluation of the Activity of Prepared Zinc Nanoparticles with Extracted Alfalfa Plant in the Treatment of Heavy Metals. *Baghdad Sci J*. 2022; 19(6): 1399-1399. <https://dx.doi.org/10.21123/bsj.2022>.
8. Singh R, Singh S. Nanomanipulation of consumer goods: effects on human health and environment. In *Nanotechnology in Modern Animal Biotechnology*; Springer. 2019; 221-254. https://doi.org/10.1007/978-981-13-6004-6_7
9. Khan I, Saeed Kh Khan I. Nanoparticles: Properties, applications and toxicities, *Arab J Chem*. 2019; 12(7): 908-931. <https://doi.org/10.1016/j.arabjc.2017.05.011>
10. Didegah F, Thelwall M. Determinants of research citation impact in nanoscience and nanotechnology. *J Assoc Inf Sci Technol*. 2013; 64(5): 1055-1064. <https://doi.org/10.1002/asi.22806>
11. Alsahib SA. Characterization and biological activity of some new derivatives derived from sulfamethoxazole compound. *Baghdad Sci J*. 2020; 17(2): 471-480. <http://dx.doi.org/10.21123/bsj.2020.17.2.0471>.
12. Bayda S, Adeel M, Tuccinardi T, Cordani M, Rizzolio F. The history of nanoscience and nanotechnology: from chemical-physical applications to nanomedicine. *Molecules*. 2020; 25(1):112. <https://doi.org/10.3390/molecules25010112>.
13. Rajagopal G, Nivetha A, Ilango S, Muthudevi GP, Prabha I, Arthimanju R. Phytofabrication of selenium nanoparticles using Azollapinnata: Evaluation of catalytic properties in oxidation, antioxidant and antimicrobial activities. *J Environ Chem Eng*. 2021 Aug 1; 9(4): 105483. <https://doi.org/10.1016/j.jece.2021.105483>
14. Venkat KS, Rajeshkumar S. Plant-Based Synthesis of Nanoparticles and Their Impact. In *Nanomaterials in Plants, Ch 2, Algae and Microorganisms*. 2018; 1: 33-57. <https://doi.org/10.1016/B978-0-12-811487-2.00002-5>.
15. Lashin I, Hasanin M, Hassan SAM, Hashem AH. Green biosynthesis of zinc and selenium oxide nanoparticles using callus extract of *Ziziphus spinachristi*: characterization, antimicrobial, and antioxidant activity. *Biomass Convers Biorefin*. 2023; 13: 10133-10146. <https://doi.org/10.1007/s13399-021-01873-4>
16. Siddiqi KS, Husen A. Green synthesis, characterization and uses of palladium/platinum nanoparticles. *Nanoscale Res Lett*. 2016; 11: 1-13. <https://doi.org/10.1186/s11671-016-1695-z>.
17. Aboyewa JA, Sibuyi NRS, Meyer M, Oguntibeju OO. Green Synthesis of Metallic Nanoparticles Using Some Selected Medicinal Plants from Southern Africa and Their Biological Applications. *Plants* 2021, 10: 1929. <https://doi.org/10.3390/plants10091929>.
18. da Silva AF, Fagundes AP, Macuvelo DL, de Carvalho EF, Durazzo M, Padoin N, et al. Green synthesis of zirconia nanoparticles based on *Eucleanatalensis* plant extract: Optimization of reaction conditions and evaluation of adsorptive properties. *Colloids Surf A Physicochem Eng Asp*. 2019 Dec 20; 583: 123915. <https://doi.org/10.1016/j.colsurfa.2019.123915>
19. Abdul Kareem L K , Radhi I M, Mohammed S S . Biological activity of complexes of some amino acid: Review. *Indian J Forensic Med Toxicol*. 2020; 14(4): 2254-2261. <https://doi.org/10.37506/ijfnt.v14i4.11888>.
20. Alagarsamy A, Chandrasekaran S, Manikandan A. Green synthesis and characterization studies of biogenic zirconium oxide (ZrO₂) nanoparticles for adsorptive removal of methylene blue dye. *J Mol Struct*. 2022; 1247: 131275. <https://doi.org/10.1016/j.molstruc.2021.131275>.
21. Kumaresan M, Anand KV, Govindaraju K, Tamilselvan S, Kumar VG. Seaweed *Sargassum wightii* mediated preparation of zirconia (ZrO₂) nanoparticles and their antibacterial activity against gram positive and gram negative bacteria. *Microb Pathog*. 2018; 124: 311-5. <https://doi.org/10.1016/j.poly.2009.06.032>.
22. Karunakaran G, Suriyaprabha R, Manivasakan P, Yuvakkumar R, Rajendran V, Kannan N. Screening of in vitro cytotoxicity, antioxidant potential and bioactivity of nano- and micro-ZrO₂ and-TiO₂ particles. *Ecotoxicol Environ Saf*. 2013; 93: 191-7. <https://doi.org/10.1016/j.poly.2009.06.032>
23. Ghani S, Rafiee B, Bahrami S, Mokhtari A, Aghamiri S, Yarian F. Green synthesis of silver nanoparticles using the plant extracts of *vitex agnus castus* L: An ecofriendly approach to overcome antibiotic resistance. *Int J Prev Med*. 2022 Oct; 13: 133. http://10.4103/ijpvm.ijpvm_140_22.
24. Salavati-Niasari M, Dadkhah M, Davar F. Pure cubic ZrO₂ nanoparticles by thermolysis of a new precursor. *Polyhedron*. 2009 Sep 23; 28(14): 3005-9. <https://doi.org/10.1016/j.poly.2009.06.032>
25. Mahdi S H, Abdul Kareem, LK. Synthesis, characterization, anticancer and antimicrobial studies of metal nanoparticles derived from Schiff base complexes. *Inorg. Chem. Commun*. 2024; 156(112524). <https://doi.org/10.1016/j.inoche.2024.112524>
26. Al-Zaqri N, Muthuvel A, Jothibas M, Alsalme A, Alharthi FA, Mohana V. Biosynthesis of zirconium oxide nanoparticles using *Wrightiatinctoria* leaf extract: Characterization, photocatalytic degradation and antibacterial activities. *Inorg Chem Commun*. 2021; 127: 108507. <https://doi.org/10.1016/j.inoche.2021.108507>

27. Salem SS, Fouda Amr. Green synthesis of metallic nanoparticles and their prospective biotechnological applications: an overview. *Biol Trace Elem Res.* 2021; 199 (1): 344-370. <https://doi.org/10.1007/s12011-020-02138-3>
28. Sigwadi R, Mokhotjwa SD, Touhami M, Patrick N. Effect of synthesis temperature on particles size and morphology of zirconium oxide nanoparticle. *Nano Res.* 2017; 50: 18-31. <https://doi.org/10.4028/www.scientific.net/JNanoR.50.18>
29. Abeer BS, Al-Shmgani HS, Khalil KA, Mohammed HA. Evaluation of the potential protective role of galangin associated with gold nanoparticles in the histological and functional structure of kidneys of adult male albino mice *Mus musculus* administration with carbon tetrachloride. *Ibn al-Haitham J Pure Appl Sci.* 2023; 36(3): 72-84. <http://doi.org/10.30526/36.3.3250>
30. Habis C, Zaraket J, Aillerie M. Transparent Conductive Oxides. Part II. Specific Focus on ITO, ZnO-AZO, SnO₂-FTO Families for Photovoltaics Applications. *Defect Diffus Forum.*2022; 417(4): 257-272. <https://doi.org/10.4028/p-6fqmfi> .
31. Zhu W, Wu Y, Zhang Y. Synthesis and characterisation of superhydrophobic CNC/ZnO nanocomposites by using stearic acid. *Micro Nano Lett.*2019; 14(13): 1317-1321. <https://doi.org/10.1049/mnl.2019.0335> .
32. Mohan B, Shaalan N. Synthesis, Spectroscopic, and Biological Activity Study for New Complexes of Some Metal Ions with Schiff Bases Derived From 2-Hydroxy Naphthaldehyde with 2-amine benzhydrazide. *Ibn al-Haitham J Pure Appl Sci.* 2023; 36(1): 208-224. <http://doi.org/10.30526/36.1.2978>
33. Nisar MF, Khadim M, Rafiq M, Chen J, Yang Y, Wan CC. Pharmacological properties and health benefits of eugenol: a comprehensive review. *Oxid Med Cell Longev.* 2021; 2021(2): 1-14. <https://doi.org/10.1155/2021/2497354>.
34. Khalaf RL, Ahmed EM, Mathkor TH, AL-Zubaidi HY. Synthesis of Silver Nanoparticles Using L. Rosa Flowers Extracts: Thermodynamic and Kinetic Studies on the Inhibitory Effects of Nanoparticles on Creatine Kinase Activity. *Iraqi J Sci.* 2021; 62(8): 2486-500. <https://doi.org/10.24996/ijs.2021.62.8.1>
35. Mohammed DB, Abbas AH, Ali AMA, Abed EH. Biodegradation of Anthracene Compound by Two Species of Filamentous Fungi. *Baghdad Sci J.* 2018; 5(1): 43-47. <http://dx.doi.org/10.21123/bsj.2018.15.1.0043> .
36. Baqer SR, Alsammaraie AMA, Alias M, Al-Halbosi MM, Sadiq AS. In Vitro Cytotoxicity Study of Pt Nanoparticles Decorated TiO₂ Nanotube Array. *Baghdad Sci J.* 2020; 17(4): 1169-1169. <https://doi.org/10.21123/bsj.2020.17.4.1169>.
37. Wasly HS, El-Sadek MA, Henini M. Influence of reaction time and synthesis temperature on the physical properties of ZnO nanoparticles synthesized by the hydrothermal method. *Appl Phys.* 2018; 124:1-12. <https://doi.org/10.1007/s00339-017-1482-4>
38. Tharp, W F, Karem, L K A. Ewies F. Ewies. Green Synthesis, Characterization, Antimicrobial and Anticancer Studies of Zirconium Oxide Nanoparticles Using Thyme plant Extract. *Mor. J. Chem.* 2024; 12(2): 643-656. <https://doi.org/10.48317/IMIST.PRSM/morjchem-v12i2.45880>.
39. Omanović-Miklićanin E, Badnjević A, Kazlagic A, Hajlovac M. Nanocomposites: A brief review. *Health Technol.* 2020; 10(1): 51-9. <https://doi.org/10.1007/s12553-019-00380-x>
40. Mahmoud WH, Deghadi RG, Mohamed GG. Metal complexes of ferrocenyl-substituted Schiff base: Preparation, characterization, molecular structure, molecular docking studies, and biological investigation. *J Organomet Chem.* 2020; 917: 121113. <https://doi.org/10.1016/j.jorganchem.2020.121113>
41. Zari AT, Zari TA, Hakeem KR. Anticancer Properties of Eugenol: A Review. *Molecules.* 2021; 26(23):7407. <https://doi.org/10.3390/molecules26237407>
42. Mohammed SS, Karem LKA, Salman SA, Al-Darwesh MY. Spectroscopic, Thermodynamic and Kinetic Studies of Ligand Complexes Derived from 2-Aminothiophenol. *Biochem Cell Arch.* 2020; 20(2): 6329-6334.
43. Alwash A. The green synthesise of zinc oxide catalyst using pomegranate peels extract for the photocatalytic degradation of methylene blue dye. *Baghdad Sci J.* 2020; 17(3): 787- 794. <http://dx.doi.org/10.21123/bsj.2020.17.3.0787>.

دراسة سمية وفعالية جسيمات اوكسيد الزركونيوم النانوية المحضرة من مستخلص نبات كف العذراء

صبا حربي مهدي¹، لقاء خالد عبد الكريم²

¹مديرية تربية بغداد، الرصافة الأولى، وزارة التربية، بغداد، العراق.
²قسم الكيمياء، كلية التربية للعلوم الصرفة ابن الهيثم، جامعة بغداد، بغداد، العراق.

الخلاصة

في الدراسة الحالية، تم تصنيع جسيمات ZrO_2 النانوية باستخدام مستخلص نباتي مشتق من نبات *Vitex agnus castus*، ووسط قلوي مثل هيدروكسيد الصوديوم. تم استخدام أسلوب التخليق الحيوي لتحضير جزيئات أوكسيد الزركونيوم النانوية لهذا المشروع البحثي. تتميز هذه الطريقة عن غيرها بسبب فعاليتها من حيث التكلفة وبساطتها وقلة المخاطر المحتملة. وتم تشخيص العينات المحضرة باستخدام المجهر الإلكتروني النافذ TEM، المجهر الإلكتروني الماسح SEM، التحليل الطيفي بالأشعة تحت الحمراء بتحويل فورييه FT-IR، التحليل الطيفي فوق البنفسجي المرئي، حيود الأشعة السينية، والتحليل الطيفي للأشعة السينية المشتتة من الطاقة EDX. تم تحديد حجم البلورة باستخدام حيود الأشعة السينية من معادلة ديبي-شيرر بقيمة 26.37 نانومتر. تم استخدام المجهر الإلكتروني الماسح والمجهر الإلكتروني النافذ للتأكد من حجم جسيمات ZrO_2 النانوية. في هذه الدراسة، أظهرت هذه الجسيمات النانوية مستويات متفاوتة من النشاط ضد نوعين من البكتيريا إيجابية الجرام (*Streptococcus pneumoniae* و *Staphylococcus aureus*)، ونوعين من البكتيريا السالبة الجرام (*Proteus mirabilis* و *Escheria coli*)، ونوع واحد من الفطريات وهو *Candida*. ومن المثير للاهتمام، أنه تم الكشف عن الإمكانات المضادة للسرطان لجسيمات أوكسيد الزركونيوم النانوية المركبة من خلال اختبار MTT بتركيز متنوع لسرطان الرئة A549 من خط الخلية. وأظهرت نسبة التثبيط زيادة مع زيادة التركيز. إن حساب تثبيط نصف الخلايا IC50، والذي كان يساوي (58.4 ملغم/مل)، يشير إلى أن جزيئات أكسيد الزركونيوم النانوية لديها القدرة على الاستفادة منها في علاج السرطان.

الكلمات المفتاحية: مضادات البكتيريا، طريقة التخليق الحيوي، الخط الخلوي A549، الجسيمات النانوية، أوكسيد الزركونيوم.